The Trigger System of the MAGIC Telescope

R. Paoletti, R. Cecchi, D. Corti, M. Mariotti, R. Pegna and N. Turini

Abstract— **The MAGIC telescope aims at the detection of very low energy gamma rays ($E > 10$ GeV) through the atmospheric emission of Cherenkov light. The high background rate originated by the night sky background (NSB), muons, hadronic showers and bright stars sets a seriuos challenge to this goal. Application of topological selection cuts at trigger level can have a big impact on the background reduction allowing the telescope to operate at lower thresholds and reducing the minimum detectable energy. The trigger of the MAGIC telescope is a two-level system following a pipeline philosophy, similar to those adopted in the high energy experiments. Operative since october 2002, the trigger system has been a key point in the commissioning of the MAGIC telescope that is now taking data. The trigger hardware is described in detail.**

Index Terms— **Astroparticle Physics, Astrophysics, Imaging Air Cherenkov Telescope, Trigger**

I. Introduction

THE MAGIC (Major Atmospheric Gamma Imaging Cherenkov) telescope is a second generation ground telescope that aims to measure low energy gamma-initiated showers ($E \approx 30$ GeV) by looking at the Cherenkov light emitted in the atmosphere [1]. The motivation to push for a low energy threshold telescope was the fact that first generation ground telescopes were able to confirm only a very small number of the sources detected by the EGRET satellite. To cover this unexplored energy range a new low threshold IACT telescope was designed by making use of new technological improvements. The shower signal is contaminated by background events due to various sources: hadronic showers, local muons, Night Sky Background (NSB), moon light and bright stars in the field of view of the camera. Simple topological trigger schemes looking for adjacent triggered pixels had been already implemented in previous Cherenkov telescope to limit the accidental trigger rate due to NSB events [2]. In addition to this, the trigger system of the MAGIC telescope is a true topological trigger that can apply sophisticated selections.

II. The Telescope

Located at the Observatorio Roque de los Muchachos (island of La Palma, Islas Canarias), the building of the telescope frame began in September 2001 and the whole frame structure was finished after few months (December 2001). The 17 m diameter $f/D = 1$ telescope frame is made by a nest of carbon fiber tubes specifically designed to achieve stiffness and light weight, about 20 tons, that add to the undercarriage weight to give a total weight of 40 tons (see fig. 1).

Fig. 1. The MAGIC telescope. The reflective surface has been completed in August 2004. On the left is the telescope tower, used to access the camera.

The reflective mirror surface of the MAGIC telescope has a parabolic shape to minimize the time spread of arrival photons produced by the Cherenkov flashes. The study of the time structure can contribute to a better separation between hadron– and gamma–initiated showers as well as to disentangle the effect of NSB light.

III. The Camera

The MAGIC camera has 1.5 m diameter, 450 kg weight and 3-4° field of view. The inner hexagonal area is composed by 397 hemispherical photomultipliers (PMT) (Electron Tubes 9116A, 1" diameter) surrounded by 180 PMTs (ET 9116B, 1.5" diameter). The time response FWHM is below 1 ns. The photocathode quantum efficiency is raised up to 30% and extended to the UV by a special coating of the surface using wavelength shifter (figure 2). Each PMT is connected to an ultra-fast low-noise transimpedance pre-amplifier. Winston cones are used to collect light on the photocathode and to enhance the probability to double cross the photocathode for large acceptance angles. The camera was commissioned in March 2003 and first starlight using DC current readout was recorded after few days.

The signals from the PMTs are amplified inside the camera enclosure and transmitted over 162 m long optical fibers using Vertical Cavity Emitting Laser Drivers (VCSELs, 850 nm wavelength) to reduce the weight and size of standard copper cables and to minimize the electromagnetic noise on the lines. In the electronics room the signal is split into two branches. The first branch passes through a software adjustable threshold discriminator that generates a digital signal for the trigger

Manuscript received October 29, 2004.

R. Cecchi, R. Paoletti, R. Pegna and N. Turini are with University of Siena and I.N.F.N. Sezione di Pisa.

D. Corti and M. Mariotti are with University of Padova and I.N.F.N. Sezione di Padova.

Fig. 2. View of the MAGIC camera. The photomultipliers are mounted on a hexagonal structure. On some photomultipliers the light collector has been removed, the wavelength shifter deposited on the photocathodes is clearly visible.

system. The second branch is stretched to 6 ns FWHM, amplified and sent to the readout system for digitization.

IV. The Trigger

The actual rate of noise due to night sky background depends on the threshold applied on discriminators and the logic used in the trigger. The night sky background rate was measured in La Palma to be 0.9 photons/ns/pixel. The expected rate with four-fold next-neighbor logic is around 2 kHz, for a 2 photoelectrons/pixel threshold. Other sources of noise are bright stars that should be masked at trigger level, and hadronic showers and muons that may contribute up to few tens of kHz to the total rate. It is required to mask bright stars and perform a simple gamma-hadron separation to keep the acquisition rate below 1 kHz.

Since MAGIC will perform different type of observations, like sources near or at large zenith angles and gamma bursts – either with the source centered on the camera or not – a large trigger flexibility is required. Moreover, the MAGIC data acquisition samples a time slice of 80 ns using 300 MHz Flash ADCs, and stores the digitized information in a 5 ms deep FIFO buffer. Therefore, the trigger should perform its analysis in less than 5 ms.

The trigger area is restricted to the 325 pixels of the camera inner region. Trigger cells ("macrocells") are defined by cells of 37 pixels mutually overlapping (see fig. 3). This particular overlap has been chosen to ensure an efficient coverage of all the logic combinations over the trigger area.

The trigger system is based on two pipelined levels [3], following a philosophy similar to the systems used in high energy physics experiments. Level 1 fast n-fold (n=2–5) next neighbor logic is very effective in the rejection of background light while Level 2 pattern recognition is be used to mask bright stars or to perform a preliminary event selection at trigger level. The trigger system can work up to a maximum input rate frequency of 10MHz.

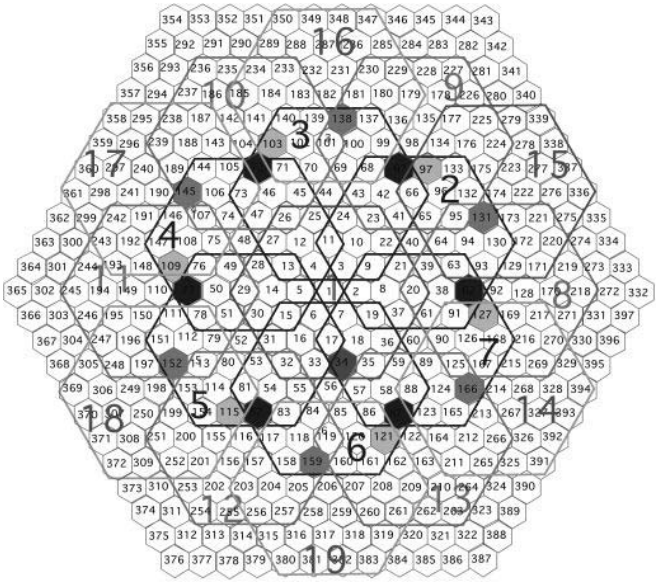

Fig. 3. The trigger area is restricted to the camera inner region. Trigger cells are mutually overlapping to ensure an efficient coverage of all logic combinations.

A. The Level 1 Trigger

The digital information coming from the receiver boards is shared by the Level 1 boards by means of a custom backplane that has the purpose to split and distribute this information to the other boards (see fig. 4). A lot of care was put in the design and layout of the backplane since the overall time jitter must be kept under one nanosecond.

The Level 1 boards use ALTERA EPLD128ATC100-7 Programmable Logic Devices (PLD) to look for n next neighbours in tight time windows in any of the 19 overlapping trigger cells (see fig. 5).

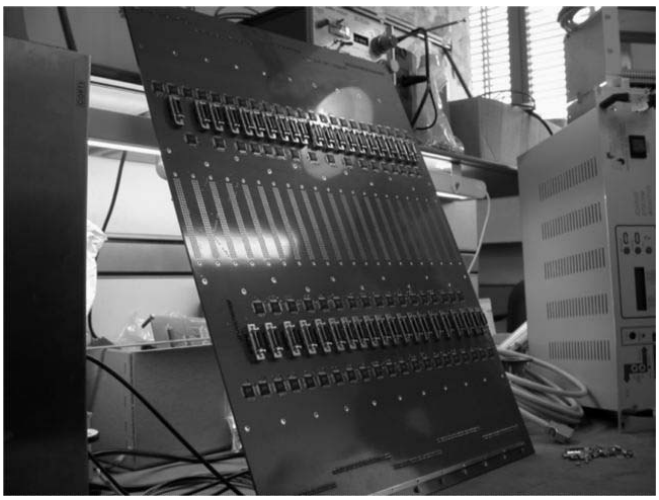

Fig. 4. Level 1 backplane. The connectors for the input signal coming from the receiver boards are visible while individual trigger boards are connected to the center (not yet mounted).

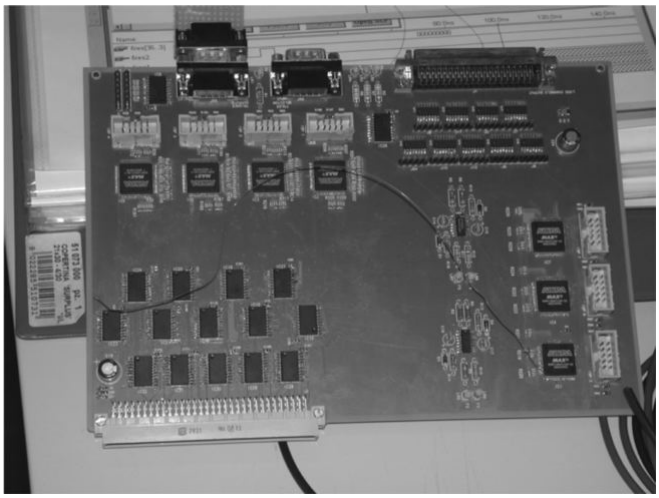

Fig. 5. Level 1 trigger board. Shown are the PLDs used for logic combinations.

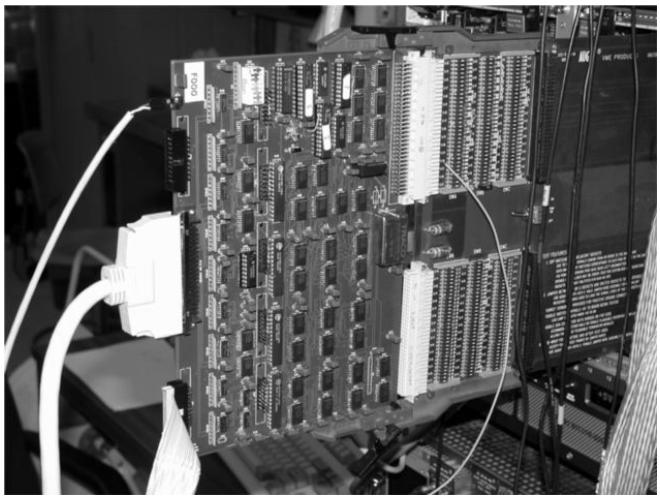

Fig. 6. One of the SMART boards used in the Level 2 trigger.

Internal delay in the combinatorial array of the devices was carefully simulated and studied. It turned out to be better than one nanosecond as required by the Level 1 specifications and independent from the route of the signals if the all sets of equation can be written in a single macro-cell of the PLD.

Inside every board, combinations of n neighbour pixels (n=2–5) are computed by equations directly implemented in the programmable logic. The choice between one of the four multiplicity configurations is remotely performed by software.

The Level 1 trigger also latches the complete pixels configuration in an output buffer so that, when a given multiplicity logic is satisfied in any of the trigger cells, the whole digital information is transmitted to the second level for further selection. The overall time delay of Level 1 is measured to be about 80 ns. The input rate per pixel can exceed the MHz range depending on the level of the discriminators thresholds. In standard conditions, a Level 1 rate of the order of few kHz or less is expected corresponding to a rejection factor between 10^3 and 10^4.

B. The Level 2 Trigger

The second level trigger consists of a first stage of 19 VME programmable modules, called SMART (see fig. 6), where the digital information for each trigger cell is split into three 12 channels, mapped in Look-Up Tables (LUT). Each LUT is made by a 4096 bytes static memory in which the 12 address bits are direclty connected to the inputs. Every input configuration is seen at the input of the three LUTs as three independent configuration sets, i.e. 3×2^{12} combinations instead of the total 2^{36} ones. The selection criteria are coded in the 5 less significant bits (LSB) of each memory and grouped in a 15 bits word that goes into a fourth LUT. The decision is coded in a 6 bits output word. Several outputs can be fed into other SMART modules as shown in fig. 7.

The typical transition time of a SMART module is 60 ns and the global trigger decision delay time is kept under 400 ns.

In order to monitor effectively the telescope behaviour, frequency rates for individual pixels are measured by custom VME scalers. Every board houses an Altera EPF10k200 FPGA to measure simulataneously the rates of 80 LVDS/TTL channels with 32 bit counters, up to a maximum frequency of 50 MHz. Two 64 bit special registers are used to measure the experiment live and dead times with 25 ns accuracy.

The trigger pipeline architecture reduces the system dead time practically to zero. The re-arming time of Level 1 is the only source of dead time but it can ignored since it is 0.01% at 1 kHz (only 7% at 1 MHz!).

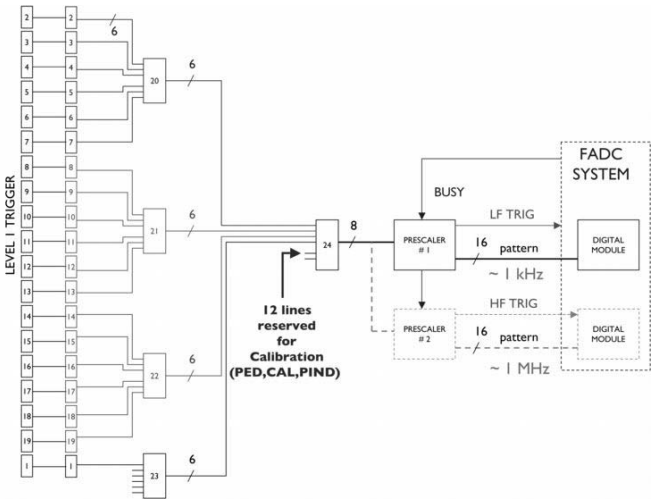

Fig. 7. Level 2 trigger system architecture. Note the possibility of implementing external signals, e.g. calibration, in the trigger system by feeding one of the SMART modules.

The trigger decision is finally coded in an 8 bit word that is sent to the VME prescaler boards and to the FADC system for event acquisition. In the prescaler board, every trigger bit can be individually prescaled by 16 bit counters (useful range 0-65535). The board can disable the counters when the data

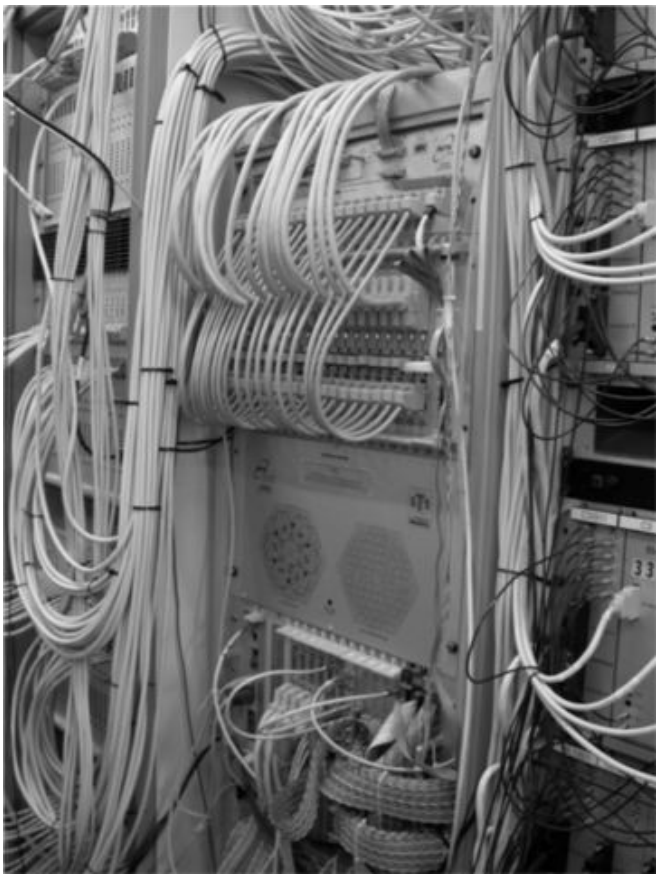

Fig. 8. Trigger electronics. The Level 1 trigger is shown on top. Input signals are cabled on the back of the rack, the output signals are transmitted over the white cables going upward. Also shown is the Level 2 crate with the CPU, some SMART modules (20–24), the prescaler and the scaler boards (from left to right). Not shown are the nineteen SMART modules directly interfacing with Level 1.

acquisition system is busy ("dead time"). Twelve lines are reserved for utility signals (see fig. 7), like random triggers or dedicated signals coming from the calibration system. Since these signals are entering in the Level 2 trigger, calibration or pedestal triggers can be selected together with shower triggers to calibrate the experiment during data taking. Coding the trigger word in 8 bits allows to work with simultaneous triggers, e.g. showers trigger can be mixed to calibration triggers.

The trigger system can be remotely programmed by a dedicated CPU located in the Level 2 VME crate.

C. Commissioning

The trigger system was commissioned in two phases. The Level 1 and a simple Level 2 version (the CPU, one SMART module and the prescaler) were installed in november 2002 while the full Level 2 system was ready by March 2003 (see fig. 8).

Several algorithms are now under study for trigger selection at Level 2. For example, the multiplicity of the cluster has been studied as a selection parameter to reject accidental NSB

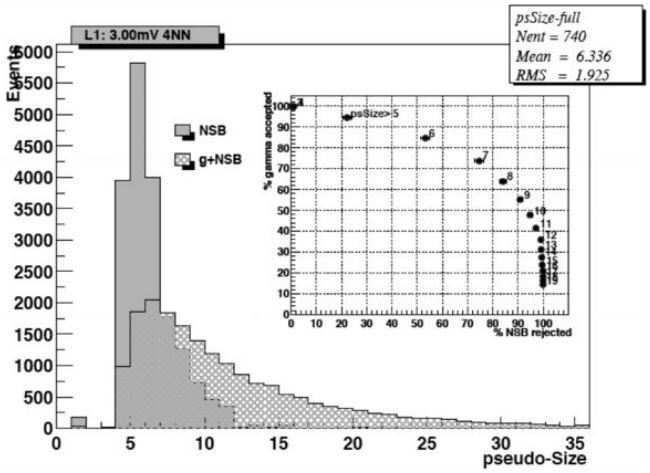

Fig. 9. Level 2 rejection of NSB. Number of events as a function the pseudo-size cut. The inset shows efficiency of accepted events vs NSB rejection.

events [4]. This method can reduce the rate of NSB events below the maximum data acquisition rate (1 kHz) and enhance the trigger collection area by 2-3 times more than the standard Level 1 trigger [5]. One of the methods under study is the "pseudo–size", that is the number of pixels belonging to a cluster (see fig. 9). For example, using a cut pseudo–size ≥ 8 more then 80% of NSB is reduced while more than 60% of the signal is kept. The trigger rate, about 3 kHz at Level 1, is reduced to 500 Hz.

V. Conclusions

The MAGIC telescope is a second generation Cherenkov telescope that incorporates many technological improvements to explore the 10-300 GeV energy window. Just after few months from installation and even if it is still in the commissionig and calibration phase, the telescope has already detected two very high energy sources, Crab and Mrk 421, with high significance.

The MAGIC telescope has the most sophisticated trigger system ever implemented in a Cherenkov telescope. The experience gained in high energy experiments has been very helpful to design the whole trigger system. Use of the fast logic at Level 1 trigger with PLDs has shown to be effective and reliable. Implementation of new selection algorithms at Level 2 are currently in use and their performances are being studied.

Acknowledgment

The authors would like to thank the Instituto de Astrofisica de Canarias (IAC) for excellent working conditions. The support of the Italian INFN, German BMBF and Spanish CICYT is gratefully acknowledged.

References

[1] C. Baixeras et al., Nucl. Instr. and Meth. A 518 (2004) 188
[2] S. M. Bradbury et al., Proc. 26^{th} ICRC, Salt Lake City (1999) OG 4.3.21
[3] D. Bastieri et al., Nucl. Instr. and Meth. A 461 (2001) 521
[4] M. Meucci et al., Nucl. Instr. and Meth. A 518 (2004) 554
[5] A. Stamerra et al., Proc. of the 28^{th} ICRC, Tsukuba (2003) p. 2959